Compact Single and Dual-Band Branch-Line Coupler with Effective Fractional Bandwidth for Wireless Communication Systems

G. Srividhya and S. Maheswari

Department of ECE
Panimalar Engineering College, Poonamallee, Chennai, Tamil Nadu 600123, India srividhyakrishiv@gmail.com, maheswarisp@yahoo.co.in

Abstract - Multiple wireless communication systems make use of a branch-line coupler (BLC), which is a passive microwave component. For the purpose of splitting and combining microwave signals, as well as providing a 90-degree phase shift between the output ports, this 4port device is made from four quarter-wavelength ($\lambda/4$) transmission lines. Having recently developed a dualband branch-line coupler (DBBLC), there has been a lot of attention paid to this development. When it comes to getting dual-band (DB) functioning of a BLC, one of the most common approaches is stub loaded transmission lines. For the BLC, stubs may be positioned either in the center of the arms or at the input of the arms. Stepped-impedance stubs, orthogonal coupled branches, and coupled lines are some of the strategies that have been shown to be effective in achieving DB functioning of a coupler. Through the utilization of the Elongated T-Shape Transmission Line (ETSTL), this work presents a one-of-a-kind design for each single-band branch-line coupler (SBBLC) and DBBLC that is of a compact proportion. Based on the information presented in this article, the SBBLC operates at a frequency of 0.9 GHz, whereas the DBBLC operates at 0.9 and 2.4 GHz. Using a fractional bandwidth (FBW) of 44%, the coupler that has been proposed is able to function at both 0.9 GHz (GSM) and 2.4 GHz (wireless). Efforts are done on reducing the size of the coupler to be ready for fabrication.

Index Terms – Branch-line coupler, dual-band branch-line coupler, single-band branch-line coupler, wireless communication systems.

I. INTRODUCTION

Branch-line couplers (BLC) are an essential component of wireless communication systems, since they enable the development of crossovers, Butler matrices (BMs), and antenna arrays. They play an important role in radio frequency (RF) and microwave systems, and they are also an essential component of wireless communication systems. There are several benefits

associated with BLC, some of which include a broad bandwidth, balanced power division, and excellent isolation between output ports. The use of microstrip or strip line transmission lines, which provide the advantages of compactness and ease of integration into microwave circuits, is often used in their construction. The compactness, fractional bandwidth (FBW), and harmonic suppression that are desired in single-band (SB) BLCs have been accomplished via the use of a number of different strategies [1–7]. A T-shaped section was used in [1] in order to accomplish the combination of small sizes and harmonic reduction. Transmission lines that are stub loaded are used for the purpose of achieving compactness, FBW, and harmonic suppression [2]. For the purpose of achieving a compact form and FBW, a T-shape with an open stub [3] and open stubs with high-low impedance [4] were used. The meander T-shaped line [5] and the symmetric structure [6] both increase isolation, return loss, and harmonic attenuation, which ultimately leads to ideal frequency response without increasing the size of the circuit. For the construction of the coupler, a microstrip-slot BLC made up of two sections was used [7]. When it comes to the miniaturization of the structure and the suppression of harmonics, low-pass filters (LPFs) [8] are used as coupler branches in a number of different designs [10] This method tends to provide satisfactory outcomes. Additionally, dual-band (DB) BLC [11–18] were explored.

In recent times, DB components have earned a great deal of attention as a result of the potential opportunities they provide for use in BM [11] and crossovers [12]. In response to this, a number of other DBBLCs have been created. A DBBLC is often created by simply exchanging every quarter-wave line from a single-band branchline coupler (SBBLC) with an equal number of DB quarter-wave blocks. This is the most common method. In order to investigate DB approaches, many strategies are used. These techniques include π -shaped lines [13], T-network [14], open-ended stub [15], coupled line [16], feature-based optimization [17], port extension [18, 19], and cross coupled [20].

Submitted On: September 3, 2024 Accepted On: May 22, 2025 Two novel couplers, a Single-Band Branch-Line Coupler (SBBLC) and a Dual-Band Branch-Line Coupler (DBBLC), are proposed using Elongated T-Shape Transmission Lines (ETSTL). The same SBBLC structure can be adapted for DBBLC operation by adjusting the electrical length of the transmission line and the open stub. Through even-odd mode analysis, the impedance values are determined. It was necessary to model, build, and evaluate a coupler operating at 0.9 GHz and 2.4 GHz using a FR4 substrate in order to verify the idea. The remaining sections of the article may be organized as follows: section II provides an illustration of the work that is suggested, section III presents the findings and discussion, and section IV draws the conclusion.

II. PROPOSED WORK

The conventional BLC is shown in Fig. 1 (a). It is composed of four branches with quarter-wavelength,

which are two series arms with an impedance of 35.35Ω and two shunt arms with an impedance of 50Ω . Using a FR4 substrate with a thickness of 1.6 mm and ε_r value of 4.4, the conventional coupler dimensions are 51.2×56.6 mm. However, the size of the device is a disadvantage of this typical technique, which is one of its problems.

A. Design of proposed SBBLC

Figure 1 (b) illustrates the construction of a SBBLC that makes use of an ETSTL with series and shunt arm. This kind of coupler is responsible for providing a connectivity between the transmission lines that have open stubs.

An Elongated T-Shape as seen in Fig. 2 comprised of three transmission lines and a stub.

The three impedances that are associated with ETSTL are Z_{1S} , Z_{1H} , and Z_{1L} . The electrical lengths that correlate to these impedances are θ_{1s} , θ_{1H} , and θ_{1L} . The

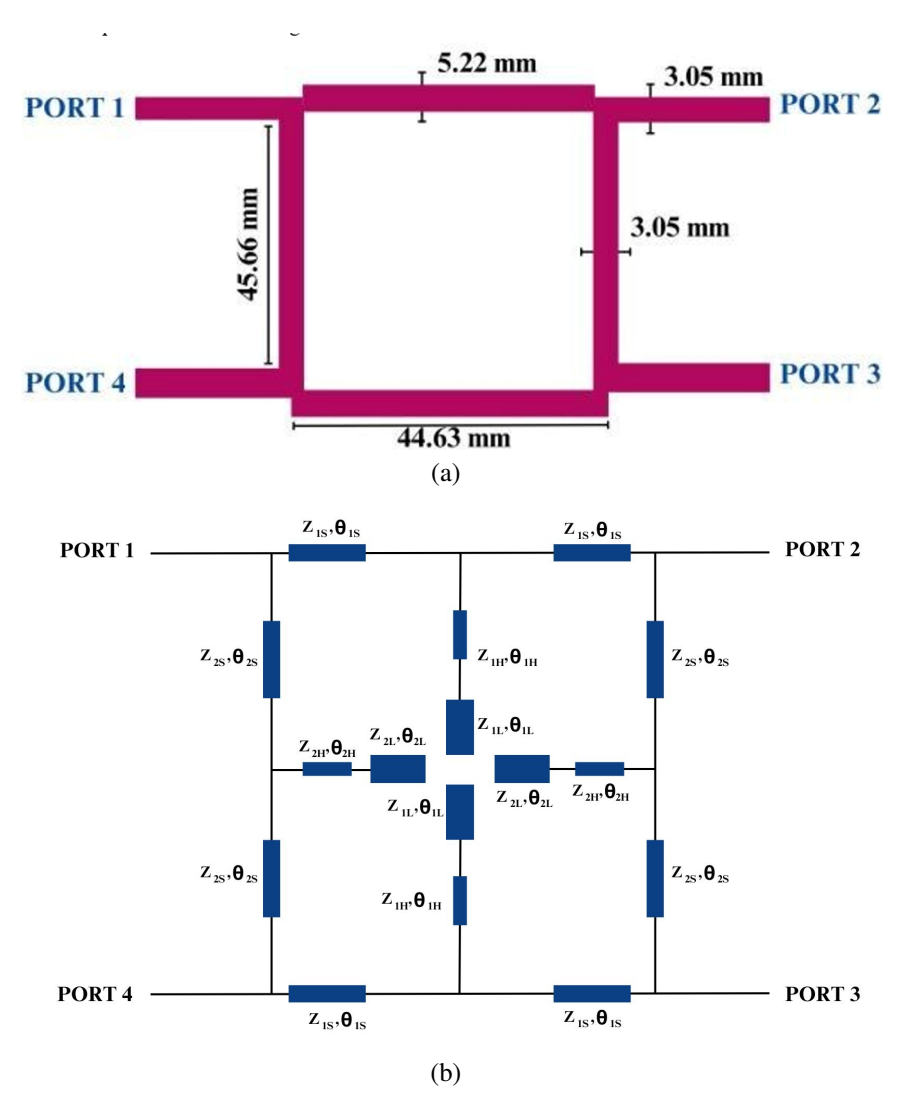


Fig. 1. Layout of (a) conventional BLC and (b) proposed SBBLC with ETSTL.

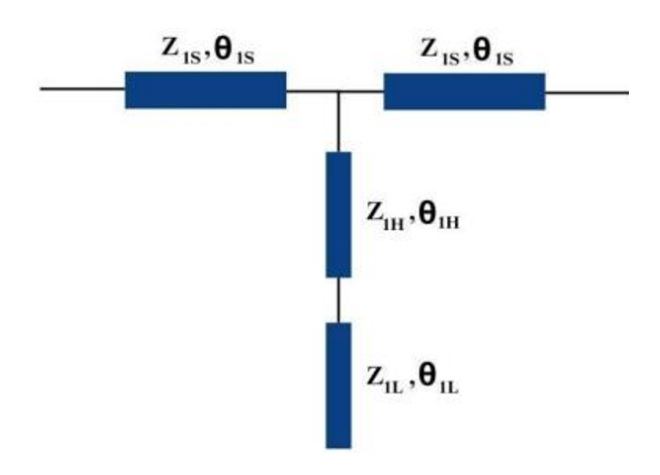


Fig. 2. Elongated T-Shape Transmission Line.

impedance of the transmission lines is represented by the symbols Z_{1S} and Z_{1H} in Fig. 2. The impedance of the stub is represented by Z_{1L} . The symbols θ_{1S} and θ_{1H} may be used to represent the electrical lengths of the transmission lines. The electrical length of the stub is represented by the symbol θ_{1L} .

B. Design of proposed DBBLC

The coupler is designed to operate at two different frequency bands, hence termed DBBLC. The operating frequencies are $f_1 = 0.9$ GHz and $f_2 = 2.4$ GHz, where the frequency ratio, p = 2.66, $\theta_1 = 49^\circ, \theta_2 = 131^\circ$.

frequency ratio,
$$p = \frac{f_2}{f_1}$$
. (1)

$$\theta_1 = \frac{\pi}{1+p}.$$
 (2)

$$\theta_2 = \frac{p\pi}{1+p}.\tag{3}$$

Frequency ratio is determined by equation (1). To further comprehend the phase connection between these frequencies, we compute two crucial angles. The first angle θ_1 simplifies to about 49° .

The second angle θ_2 is roughly 131° , calculated using equation (3). These angles, determined from the frequency ratio, reflect the phase angles connected with the frequencies, allowing for a clear understanding of their phase connection. In the proposed structure, θ_2 is divided into θ_{1H} and θ_{1L} for transmission line and stub, respectively.

C. Analysis of the proposed coupler

An even and odd mode equivalent circuit analysis is performed on the ETSTL, as can be seen in Fig. 3. When it comes to identifying the impedance and electrical lengths that are required, in order to obtain the acceptable coupling qualities, the findings of this research are useful in understanding what those dimensions are [10].

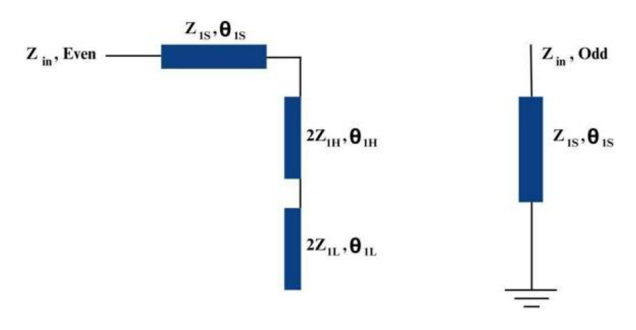


Fig. 3. Even and odd mode analysis of ETSTL.

The even and odd mode impedance of the proposed ETSTL can be written as

$$Z_{in,even} = \frac{Z_{1S}(Z_a + jZ_{1S} \tan \theta_{1S})}{Z_{1S} + jZ_a \tan \theta_{1S}}, \tag{4}$$

$$Z_{\text{in.odd}} = jZ_{1S} \tan \theta_{1S}, \tag{5}$$

where

$$Z_{a} \!\!=\! \frac{2Z_{1H}\left(Z_{b} \!+\! 2jZ_{1H} tan\theta_{1H}\right)}{2Z_{1H} \!+\! jZ_{b} tan\theta_{1H}}, \tag{4a}$$

$$Z_b = -2iZ_L \cot \theta_L. \tag{4b}$$

It is possible to express the typical transmission line for even and odd mode impedance as

$$Z_{\text{even,conv}} = -jZ_0 \cot \theta_0, \tag{5}$$

$$Z_{\text{odd.conv}} = jZ_0 \tan \theta_0.$$
 (6)

The impedance characteristics may be computed in the following manner, taking into account both the conventional design and the design that was suggested:

$$Z_{1S} = Z_0 \frac{\tan\left(\frac{\theta_0}{2}\right)}{\tan\theta_1} \tag{7}$$

$$Z_{1H} = \frac{Z_{1S}B\left[Z_{1S}\tan\theta_{1S} + Z_0\cot\left(\frac{\theta_0}{2}\right)\right]}{2A\left[Z_0\cot\left(\frac{\theta_0}{2}\right) - Z_{1S}\right]}$$
(8)

where

$$A = \tan \theta_{1H} - \frac{1}{K} \cot \theta_{1L}, \qquad (8a)$$

$$B = 1 + \frac{1}{K} \cot \theta_{1L} \tan \theta_{1H}, \tag{8b}$$

$$K = \frac{Z_{1H}}{Z_{1S}}.$$
 (8c)

Figure 4 is a representation of the equivalent series arm transmission line. The impedances that are distinctive of the series arms are what give them their identity Z_{1S} , Z_{1H} , and Z_{1L} . As a result of these arms being linked in series between the ports, it is possible to send signals or power from one port to another. In addition to being in charge of the coupling mechanism, the series arms are also responsible for determining how power is distributed among the ports.

The equivalent shunt arm transmission line is shown in Fig. 5. The shunt arms are represented by the

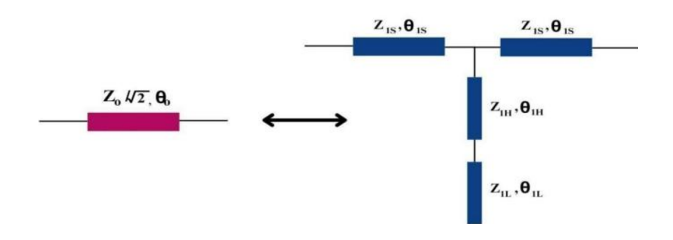


Fig. 4. Equivalent series arm transmission line.

impedances Z_{2S} , Z_{2H} , Z_{2L} . The ground reference and the series arms are linked to these arms in a parallel fashion and provide the connection. It is the shunt arms that are responsible for ensuring that the ports remain isolated and that the impedance matching that is sought is maintained. In addition to this, they further contribute to the overall coupling qualities of the coupler.

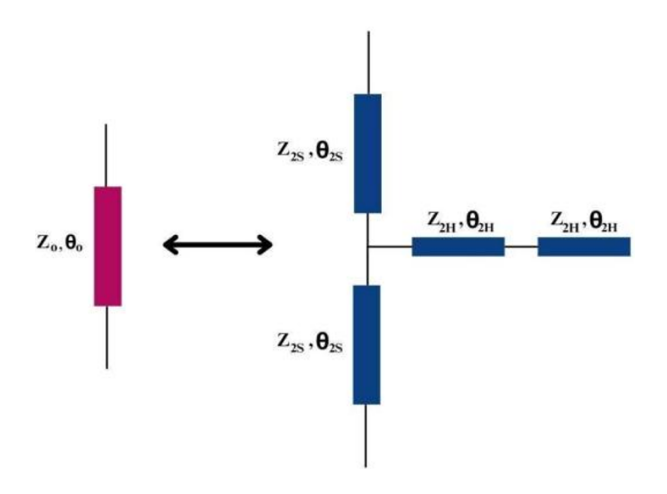


Fig. 5. Equivalent shunt arm transmission line.

The design curve for Z_{1S} , Z_{1H} is shown in Fig. 6, against the value of θ_{1S} for the series arm. To get the value of θ_{1S} , it is necessary to solve equations (7) and (8) mathematically. This allows one to derive the impedance of Z_{1S} , Z_{1H} by altering the electrical length. Under the assumption that K is equal to one, θ_{1H} is equal to θ_{1L} for 20. In order to produce an SBBLC using ETSTL on a FR4 substrate with a dielectric constant $\varepsilon_r = 4.4$ and a substrate thickness of 1.6 mm, it is necessary to replace the traditional BLC with similar ETSTL units.

Figure 6 shows the design curve for Z_{1S} , Z_{1H} versus θ_{1S} for a series arm by solving equations (7) and (8) graphically to obtain the impedance of Z_{1S} , Z_{1H} by varying the electrical length by assuming $K=1, \theta_{1H}=\theta_{1L}=20$ in order to determine the θ_{1S} value.

Figure 7 shows the design curve for Z_{2S} , Z_{2H} versus θ_{2S} for the shunt arm by solving equations (7) and (8) graphically to obtain the impedance of Z_{2S} , Z_{2H} by varying the electrical length by assuming $K=1, \theta_{2H}=\theta_{2L}=20$,

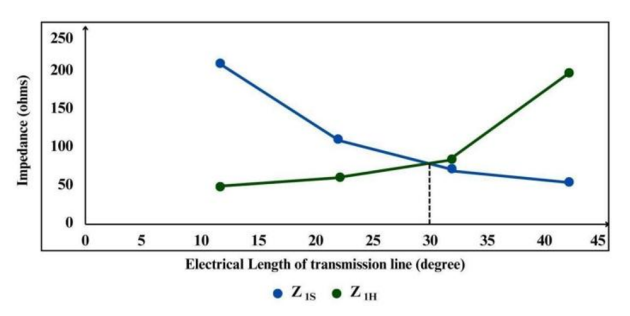


Fig. 6. Impedance versus electrical length of series SBBLC.

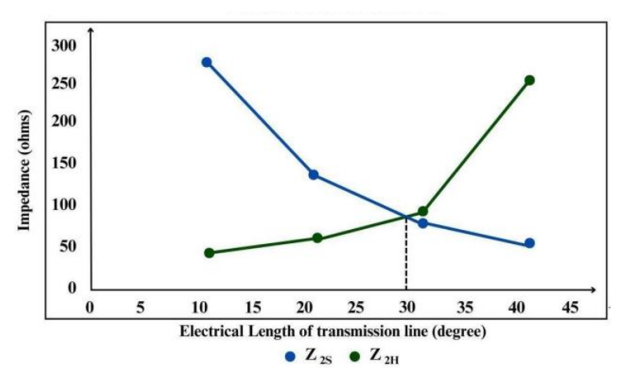


Fig. 7. Impedance versus electrical length of shunt SBBLC.

in order to determine θ_{2S} . The following values are obtained for the ETSTL for SBBLC (Series Arm), $Z_{1S}{=}61.26,\,Z_{1H}{=}69.76,\,Z_{1L}{=}61.26$ when we substitute the electrical length values as in equations (7) and (8). In same way, for shunt arm, the impedance values are $Z_{2S}{=}86.60,\,Z_{2H}{=}98.72,\,Z_{2L}{=}86.60.$ Table 1 shows the series and shunt value analysis of SBBLC.

Figure 8 (a) shows the impact of Impedance versus electrical length for series arm of DBBLC. In the equivalent series arm, the characteristics impedance of the coupler for $k=1,\ Z_{1H}$ at Z_0 tends to fall between 327Ω to $229\Omega.$ Similarly for $k=2,\ Z_{1H}$ at Z_0 tends to fall between 166Ω to 110Ω which is not feasible for fabrication because the impedance is not suitable for the FR4

Table 1: Series and shunt value analysis of SBBLC

ARM	IMPEDANCE	WIDTH	LENGTH	
AKIVI	$(\mathbf{\Omega})$	(mm)	(mm)	
SERIES	$Z_{1S} = 61.26$	2.14	15.43	
	$Z_{1H} = 69.76$	1.66	10.38	
	$Z_{1L} = 61.26$	2.14	10.28	
SHUNT	$Z_{2S} = 86.60$	1.03	15.81	
	$Z_{2H} = 98.72$	0.73	10.64	
	$Z_{2L} = 86.60$	1.03	10.54	

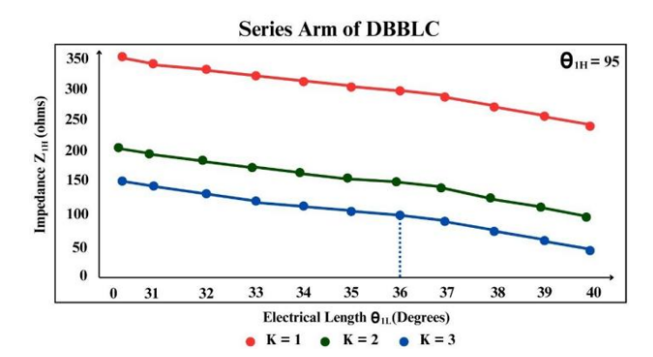


Fig. 8. (a) Impedance versus electrical length for series arm of DBBLC.

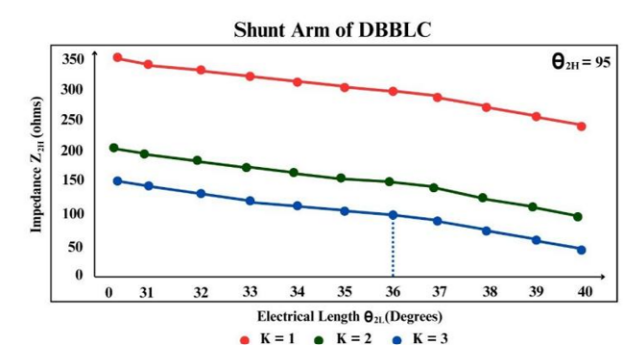


Fig. 8. (b) Impedance versus electrical length for shunt arm of DBBLC.

substrate. When $k=3,\,Z_{1H}$ at Z_0 tends to fall between 102Ω to $68\Omega\,$ at $\theta_{1H}=95$ and $\theta_{1L}\!=\!30,$ which provides the feasibility to fabricate the FR4 substrate of the proposed design.

Figure 8 (b) shows the impact of Impedance versus electrical length for shunt arm of DBBLC. In the equivalent shunt arm, the power division ratio of the equal power division coupler for k=1, Z_{2H} at Z_0 / $\sqrt{2}$ tends to fall between 475 Ω to 332 Ω . Similarly for k=2, Z_{2H} at Z_0 / $\sqrt{2}$ tends to fall between 240 Ω to 160 Ω which is not feasible for fabrication because the impedance is not suitable for a FR4 substrate. Hence, when k=3, Z_{2H} at Z_0 / $\sqrt{2}$ tends to fall between 155 Ω to 99 Ω at θ_{2H} = 95 and θ_{2L} = 30 provides the feasibility to fabricate in the FR4 substrate of the proposed design. The overall parameter value obtained on series and shunt arm for DBBLC are illustrated in Table 2.

III. PERFORMANCE ANALYSIS

Evaluation of the designed architecture is done in this section. Commercial electromagnetic simulation software ADS is used for the optimization of physical parameters. For the conventional BLC, characteristic impedance of the shunt arm is 50, and impedance of the series arm is 35.35Ω .

Table 2: Calculated parameter values of DBBLC

	Circuit	Structure Parameters
	Parameters (Ω)	(mm)
		$l_1 = 30.86 \text{ mm}$
		$l_2 = 49.97 \text{ mm}$
Series	$Z_{1S} = 30.729$	$l_3 = 17.69 \text{ mm}$
	$Z_{1H} = 83.91$	$w_1 = 6.35 \text{ mm}$
	$Z_{1L} = 30.729$	$w_2 = 1.11 \text{ mm}$
		$w_3 = 6.35 \text{ mm}$
		$l_4 = 49.24 \text{ mm}$
		$l_5 = 51.21 \text{ mm}$
	$Z_{2S} = 43.46$	$l_6 = 18.09 \text{ mm}$
Shunt	$Z_{2H} = 118.60$	$w_4 = 3.83 \text{ mm}$
	$Z_{2L} = 43.46$	$w_5 = 0.42 \text{ mm}$
		$w_6 = 3.83 \text{ mm}$

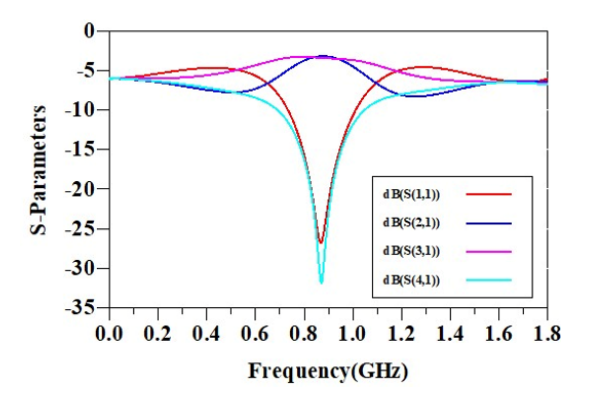


Fig. 9. Simulation result of conventional BLC.

Figure 9 shows the S-parameters of the conventional BLC. From the plot, the output characteristics of the BLC can be observed, including the insertion loss, coupling, isolation, and return loss at the output ports.

A. Simulation result of proposed SBBLC

Figures 10 (a) and (b) show the simulation results of SBBLC. Ideally, S_{11} and S_{41} should be greater than -15 dB and the proposed SBBLC has achieved -24.8 dB and -22.4 dB, respectively.

Ideally, S_{21} and S_{31} should be -3 dB and the proposed SBBLC achieves -3.5 dB and -3.2 dB, respectively. When compared to a conventional coupler, SBBLC achieved 55% size reduction and 33% FBW.

B. Simulation result of proposed DBBLC

For the DBBLC, the center frequency is located at 0.9 to 2.4 GHZ, maximal measured insertion losses |S21|/|S31| are -3.5 to -4.7 dB and -3.6 to -3.7 dB, respectively.

 S_{11} and S_{41} should be greater than -15 dB and the proposed DBBLC has achieved -16.7 to -18.4 dB and -17.6 to -18.1 dB for 0.9 GHz and 2.4 GHz, respectively.

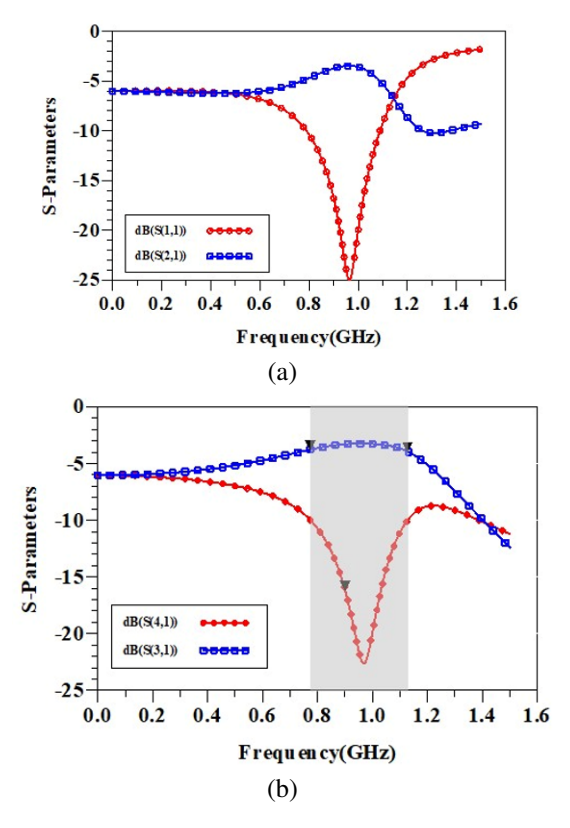


Fig. 10. (a) Simulation result of Return Loss S_{11} and Insertion Loss S_{21} of SBBLC and (b) simulation result of Isolation S_{41} and Coupling S_{31} of SBBLC.

Similarly, S_{21} and S_{31} should be -3 dB and the proposed DBBLC has achieved -3.5 to -4.7 dB and -3.6 to -3.7 dB for 0.9 GHz and 2.4 GHz, respectively.

FBW achieved nearly 400 MHz (44%). The size of the proposed coupler is reduced by 67% compared to the conventional structure.

Suggested BLC simulated S-parameters are shown in Figs. 11 (a) and (b). The down peaks show the midpoint frequencies of the two comparison pass bands. The most that may be seen in the amplitude imbalance between the output ports is 0.3 dB. At mid-frequency ranges, isolation loss, and return loss are both significantly below -20 dB.

Figure 12 shows the layout of the DBBLC. Following fabrication (Fig. 13) and measurement of the coupler prototype, the suggested design idea is evaluated to see whether it is feasible. Both the SNA4400 network analyzer and ADS Keysight were used to do simulations and analyses on the proposed DBBLC.

From the above discussions, the proposed model has dimensions of $0.29\lambda g \times 0.32\lambda g$ (λg is the full transmission wavelength at the center frequency).

The even-odd mode analysis and practical design impedance curves provide explicit design formulae. A 0.9/2.4 GHz DBBLC is manufactured for the purpose of

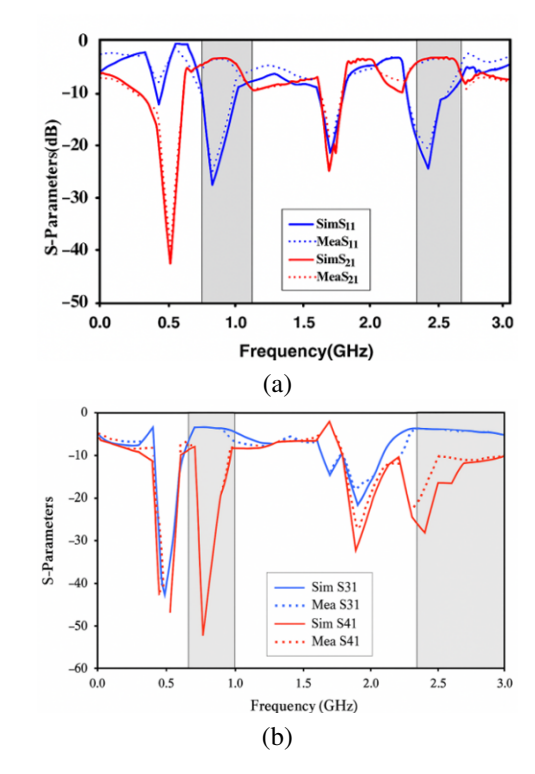


Fig. 11. (a) S_{11} and S_{21} parameter value analysis of DBBLC and (b) S_{31} and S_{41} parameter value analysis of DBBLC.

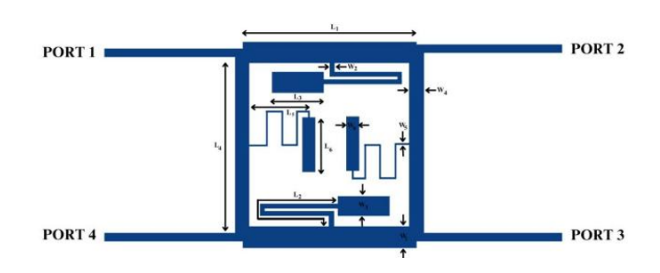


Fig. 12. Layout of the DBBLC.



Fig. 13. Fabricated prototype of the DBBLC.

verification. The findings from the simulations and the measurements are in good agreement. The coupler has an

easy-to-understand architecture with strategically placed ports, and it also provides some leeway in the design for potential other uses. Figure 14 shows the experimental setup for DBBLC.

Compared with other works (see Tables 4 and 5), the suggested architecture output performs better than other



Fig. 14. Experimental setup for DBBLC.

Table 3: Proposed architectures performance comparison

	F	Return	Isolation	Size	FBW	
	(GHz)	Loss (dB)	(dB)	(λg^2)	(%)	
SBBLC	0.9	24.83	24.47	$0.17 \times$	33	
				0.18		
DBBLC	0.9/2.4	16.7/	17.8/18.1	$0.28 \times$	44	
		18.41		0.32		

Table 4: Comparison between proposed SBBLC and others

Ref.	F	Return	Isolation	Size	Size	FBW
	(GHz)	Loss	(dB)	(λg^2)	Reduction	(%)
		(dB)			(%)	
[2]	2.45	<20	28	-	29	50
[3]	3.55	30.69	29.28	0.27	-	32.2
				$\times 0.16$		
[4]	2.45	21.7	36.2	-	64.21	22.08
[6]	2.82	29.5	31.3	0.29	-	-
				$\times 0.26$		
[7]	3.5	<8	<11	-	31	34.4
This	0.9	24.83	24.47	0.17	55	33
SBBLC				\times 0.18		

existing architectures. DBBLC exhibits significant performance slightly higher than SBBLC.

IV. CONCLUSION

In this work, two novel couplers for SBBLC and DBBLC are proposed. In addition, design equations are offered through the use of even-odd mode analysis. The results of the simulations indicate that the coupler constructed has good degrees of matching and isolation at both center frequencies. Folding the stub towards the inner section of the coupler in order to make it suitable for manufacture is one of the methods used to reduce the size of the coupler. By using a simple design formula, the coupler presented has the potential to provide the needed output at the dual frequencies stated. The architecture proposed has a number of benefits, including a small size and FBW. Both the simulated and measured results of the structures exhibit a high degree of consistency.

REFERENCES

- [1] K. V. Phani Kumar and S. S. Karthikeyan, "Miniaturized quadrature hybrid coupler using modified T-shaped transmission line for wide-range harmonic suppression," *IET Microwaves, Antennas, and Propagation*, vol. 10, no. 14, pp. 1522-1527, Nov. 2016.
- [2] W. Nie, K.-D. Xu, M. Zhou, L.-B. Xie, and X.-L. Yang, "Compact narrow/wide band branch-line couplers with improved upper-stopband," *International Journal of Electronics and Communications*, vol. 98, pp. 45-50, Jan. 2019.
- [3] A. A. Abdulbari, S. K. A. Rahim, M. Z. A. Abd Aziz, K. G. Tan, N. K. Noordin, and M. Z. M. Nor, "New design of wideband microstrip branch line coupler using T-shape and open stub for 5G application," *International Journal of Electrical and Computer Engineering*, vol. 11, no. 2, pp. 1346-1355, Apr. 2021.
- [4] M. Y. O. Elhiwaris, S. K. A. Rahim, and U. A. K. Okonkwond, N. M. Jizat, "Miniaturized size branch line coupler using open stubs with high-low impedances," *Progress in Electromagnetics Research Letters*, vol. 23, pp. 65-74, Apr. 2011.

Table 5: Comparison between proposed DBBLC and other works

Ref.	F (GHz)	Return Loss (dB)	Insertion Loss (dB)	Coupling(dB)	Isolation (dB)	PhaseDifference (deg)	Size (λg ²)	FBW(MHz)
[16]	0.756/1.42	>15	3.35/3.74	4.0/4.10	>14	87,89	-	-
[13]	0.9/2.0	26.8/35.6	3.5/3.4	3.1/3.3	23.4/27.2	-	0.79x0.1	-
[15]	0.9/1.63	>20	3.2/3.5	3.3/4.1	>14	90.3,89.2	0.53x0.34	-
[14]	0.92/2.03	Below 24/19	3.17/3.76	3.50/3.83	Below 24/19	89.1,89.6	-	-
[17]	0.92/1.9	36.4/23.5	3.18/3.37	3.14/3.46	33.8/39.8	90,90	0.18x0.15	-
[19]	1.0/2.0	36.7/25.3	3.3/3.1	3.1/3.7	32.9/29.9	90,89	-	-
[20]	0.99/1.97	35.5/24.1	3.22/2.95	3.06/3.53	32.6/22	91,90	-	-
This Work (DBBLC)	0.9/2.4	16.7/18.41	3.5/4.7	3.6/3.7	17.8/18.1	86,91	0.28x0.32	400

- [5] K.-S. Choi, K.-C. Yoon, J.-Y. Lee, C.-K. Lee, S.-C. Kim, K.-B. Kim, and J.-C. Lee, "Compact branchline coupler with harmonics suppression using meander T-shaped line," *Microwave and Optical Technology Letters*, vol. 56, no. 6, pp. 1382-1384, June 2014.
- [6] A. Rezaei and L. Noori, "Microstrip hybrid coupler with a wide stop-band using symmetric structure for wireless applications," *Journal of Microwaves, Optoelectronics and Electromagnetic Applications*, vol. 17, no. 1, Mar. 2018.
- [7] N. A. M. Shukor and N. Seman, "Enhanced design of two-section microstrip-slot branch line coupler with the overlapped $\lambda/4$ open circuited lines at ports," *Wireless Personal Communications*, vol. 88, pp. 467-478, Nov. 2015.
- [8] K. V. Phani Kumar and S. S. Karthikeyan, "Microstrip low pass filter with flexible rolloff rates," *International Journal of Electronics and Communications*, vol. 86, pp. 63-68, Jan. 2018.
- [9] S. Roshani, S. I. Yahya, S. Roshani, and M. Rostami, "Design and fabrication of a compact branchline coupler using resonators with wide harmonics suppression band," *Electronics*, vol. 11, no. 793, Mar. 2022.
- [10] F. Hosseinkhani and S. Roshani, "A compact branch-line coupler design using low-pass resonators and meandered lines open stubs," *Turkish Journal of Electrical Engineering & Computer Sci*ences, vol. 26, pp. 1164-1170, 2018.
- [11] A. M. Zaidi, M. T. Beg, B. K. Kanaujia, J. Kishor, and K. Rambabu, "A novel dual band branch line coupler and its application to design a dual band 4 X 4 Butler matrix," *IEEE Access*, vol. 8, Apr. 2020.
- [12] M. A. Maktoomi, M. S. Hashmi, and F. M. Ghannouchi, "Systematic design technique for dual-band branch-line coupler using T- and Pinetworks and their application in novel widebandratio crossover," *IEEE Transactions on Components, Packaging and Manufacturing Technology*, vol. 6, no. 5, May 2016.
- [13] X.-Y. Zhang and J.-C. Lee, "A dual-band branchline coupler with ultra-wideband harmonic suppression," *Journal of Electromagnetic Engineering and Science*, vol. 23, no. 1, pp. 57-62, Jan. 2023.
- [14] H. Zhang and K. J. Chen, "A stub tapped branchline coupler for dual-band operations," *IEEE Microwave and Wireless Components Letters*, vol. 17, no. 2, Feb. 2007.

- [15] W. Feng, X. Duan, Y. Shi, X. Y. Zhou, and W. Che, "Dual-band branch-line couplers with short/openended stubs," *IEEE Transactions on Circuits and Systems—II: Express Briefs*, vol. 67, no. 11, Nov. 2020.
- [16] W. Feng, Y. Zhao, W. Che, H. Chen, and W. Yang, "Dual-/tri-band branch line couplers with high power division isolation using coupled lines," *IEEE Transactions on Circuits and Systems—II: Express Briefs*, vol. 65, no. 4, Apr. 2018.
- [17] S. Koziel and A. Lukasiewicz, "Fast simulation-driven feature-based design optimization of compact dual-band microstrip branch-line coupler," *International Journal of RF and Microwave Computer-Aided Engineering*, vol. 26, no. 1, Jan. 2016.
- [18] M. A. Maktoomi, M. S. Hashmi, and F. M. Ghannouchi, "A dual-band port-extended branch-line coupler and mitigation of the band-ratio and power division limitations," *IEEE Transactions on Components, Packaging and Manufacturing Technology*, vol. 7, no. 8, pp. 1313-323, Aug. 2017.
- [19] H. Kim, B. Lee, and M. J. Park, "Dual-band branch-line coupler with port extensions," *IEEE Transactions on Microwave Theory and Techniques*, vol. 58, no. 3, pp. 651-655, 2010.
- [20] M. J. Park and B. Lee, "Dual-band, cross coupled branch line coupler," *IEEE Microwave and Wireless Components Letters*, vol. 15, no. 10, pp. 655-657, 2005.



G. Srividhya is currently pursuing her Ph.D. in Information and Communication Engineering at Anna University, Chennai, India. She earned her M.Tech. in VLSI Design from Bharath University, Chennai, India (2013), and B.E. in Electronics and Communication

Engineering from SCSVMV University, Kanchipuram, India (2011). She serves as Assistant Professor in the Department of Electronics and Communication Engineering at Panimalar Engineering College, Poonamallee, Chennai, India. She has published extensively in international journals and conferences. Her research interests include VLSI design, RF devices, antenna systems, artificial intelligence, and machine learning, bridging traditional electronics with emerging technologies in modern communication systems.



S. Maheswari received the Ph.D. degree in Microwave Engineering and the M.E. degree in Applied Electronics from Sathyabama Institute of Science and Technology, Chennai, India, in 2016 and 2009, respectively. She received the B.E. degree in ECE from University of Madras.

Her area of research includes microwave and millimeter wave circuits. She has more than two decades of teaching experience. Currently she is working as a Professor in Panimalar Engineering College, Chennai, India. She is a recognized supervisor for doing research in Anna University. She has published more than 30 papers in Web of Science, Scopus indexed journals, and IEEE conferences. She is a Fellow of IETE.